*Published online 11 January 2017*

*Nucleic Acids Research, 2017, Vol. 45, No. 8* ***e59***
*doi: 10.1093/nar/gkw1324*

# Sensitive and inexpensive digital DNA analysis by microfluidic enrichment of rolling circle amplified single-molecules

**Malte Kühnemund[1,2,†], Iván Hernández-Neuta[2,†], Mohd Istiaq Sharif[2], Matteo Cornaglia[3], Martin A.M. Gijs[3] and Mats Nilsson[1,2,*]**

[1]Science for Life Laboratory, Department of Immunology, Genetics and Pathology, Uppsala University, SE-751 05 Upssala, Sweden, [2]Science for Life Laboratory, Department of Biophysics and Biochemistry, Stockholm University, SE- 171 65 Solna, Sweden and [3]Laboratory of Microsystems, École Polytechnique Fédérale de Lausanne (EPFL), CH-1015 Lausanne, Switzerland

Received July 21, 2016; Revised December 13, 2016; Editorial Decision December 18, 2016; Accepted December 22, 2016

## ABSTRACT

**Single molecule quantification assays provide the ultimate sensitivity and precision for molecular analysis. However, most digital analysis techniques, i.e. droplet PCR, require sophisticated and expensive instrumentation for molecule compartmentalization, amplification and analysis. Rolling circle amplification (RCA) provides a simpler means for digital analysis. Nevertheless, the sensitivity of RCA assays has until now been limited by inefficient detection methods. We have developed a simple microfluidic strategy for enrichment of RCA products into a single field of view of a low magnification fluorescent sensor, enabling ultra-sensitive digital quantification of nucleic acids over a dynamic range from 1.2 aM to 190 fM. We prove the broad applicability of our analysis platform by demonstrating 5-plex detection of as little as ∼1 pg (∼300 genome copies) of pathogenic DNA with simultaneous antibiotic resistance marker detection, and the analysis of rare oncogene mutations. Our method is simpler, more cost-effective and faster than other digital analysis techniques and provides the means to implement digital analysis in any laboratory equipped with a standard fluorescent microscope.**

## INTRODUCTION

Nucleic acid (NA) analysis has become an important tool in research and diagnostics by enabling quantification and interrogation of their sequences down to the single base level. In the last decade, digital single-molecule detection methods, such as digital PCR (1,2), rolling circle amplification (RCA) (3,4,5), nanostring technology (6), gel- based clonal *in situ* amplification methods (7,8) and next generation sequencing (NGS) combined with unique molecular identifier tags (9), have enabled precise quantification of NAs through molecule counting. NGS-based molecule counting relies on complex library preparation schemes, and high sequencing depths are required to achieve high sensitivity. *In situ* gel-based digital analysis and RCA-in-solution methods require imaging large areas in order to detect rare molecules. Digital PCR systems are composed of several sophisticated instruments for droplet generation, PCR cycling and readout (2). Moreover, the sensitivity and multiplexing capability of commercial droplet PCR systems are limited by the total number of droplets that can be generated and analysed per run (10,11). Consequently, the need for sophisticated instrumentation and prolonged image acquisition, make digital NA analysis either expensive or time-consuming, hence limiting their broad implementation.

Contrary to the complexity of most single-molecule quantification methods, RCA amplifies a large number of circular templates in homogeneous solution. RCA products (RCPs) remain spatially separated and confined as single-stranded concatemers (3,12), collapsing into submicron-sized DNA coils that can be digitally quantified (5,13,14,15). Yet, the sensitivity of RCA-based single molecule detection assays has been greatly limited by the detection efficiency and throughput of available RCP quantification methods. In the homogeneous amplified single-molecule detection (ASMD) method (5), RCP solutions are flowed through a microfluidic channel and only a ∼0.1–3% fraction of RCPs passing through a confocal volume are detected (5,16). Alternative digital RCP quantification methods (Supplementary Table S1), aimed to detect a higher fraction of RCPs, but did not substantially improve the detection efficiency (14,15,17), leaving a gap for more efficient

*To whom correspondence should be addressed. Tel: +46 8 16 20 20; Mobile: +46 730 537 876; Email: mats.nilsson@scilifelab.se
†These authors contributed equally to this work as the first authors.

RCP read-out technologies. So far, high NA detection sensitivity using RCA-based methods could only be achieved by employing additional amplification steps through, for example, circle-to-circle amplification (18), which adds unnecessary complexity to RCA assays, and impedes their wider use and implementation.

To address these limitations, we developed a simple, yet highly efficient RCP analysis method based on microfluidic enrichment of RCPs into the field of view (FOV) of a standard fluorescence microscope. We demonstrate simple DNA preparation schemes that make this mode of digital NA analysis highly versatile and broadly applicable. As examples, we show multiplexed quantification of bacterial pathogenic DNA and associated antibiotic resistance marker genes, and provide a proof of concept for oncogene rare mutation analysis.

## MATERIALS AND METHODS

### Microfluidic chip fabrication

We have designed a multi-layer hybrid microfluidic chip that comprises four polydimethylsiloxane (PDMS) layers, a glass cover slip, a circular porous membrane and a PMMA frame (Figure 1B–D, Supplementary Figure S1). Membranes are placed between two channel layers in such a way that incoming solutions can flow through the membrane (Figure 1C and D). An O-ring structure seals the connection between the layers, by pressing the membrane against the top channel layer. Channel layers were manufactured by adhesive-tape soft lithography (19) in a glass Petri dish. Briefly, adhesive tape (Scotch 3650, 3M) was adhered to a glass Petri dish and channel masters with dimensions of 12 × 0.9 mm were cut with a blade. Unwanted surrounding tape was peeled off and remaining adhesive tape channel masters were briefly incubated at 65°C for 5 min. PDMS (Sylgard® 184, Dow Corning) was mixed in a 10:1 ratio (w/w) with the cross-linker, poured on top of the mold, degassed in a vacuum chamber for 1 h and cured at 65°C for 8 h. Cured PDMS layers with channel structures were cut in a rectangle of 34 × 24 mm and peeled off from the mold. 0.75 mm access holes for tubing connections and 1.5 mm vertical channels were opened with biopsy punchers (Harris Unicore). The middle layer was fabricated likewise but using a Petri dish without channel structures and a higher volume of PDMS to achieve 1.5 mm thickness. A 0.75 mm tubing connection was punched, as well as a vertical channel with 4 mm diameter in the middle that serves to harbour the membrane. The O-ring was fabricated by punching a 2 mm diameter opening into the same 4 mm diameter piece that was removed from the middle layer. The O-ring was aligned and glued to the lower channel layer with liquid PDMS and incubation at 65°C for 30 min. A 4 mm thick PDMS bottom layer was fabricated, into which 0.75 mm tube connections were punched. The thick bottom layer serves to align and connect the other 3 layers with 1/16 PEEK tubings (IDEX). A detailed drawing of the chip architecture with dimensions is depicted in Supplementary Figure S1. We want to highlight that the chip dimensions, including layer and channel sizes, are not crucial for successful outcome and may be modified. Critical parameters are thickness of the top channel layer, which should be fabricated as thin as possible in order to minimize the distance between objective and membrane, and the diameter of the vertical channel, which determines the area onto which the RCPs are enriched. We used a 1.5 mm diameter vertical channel, which corresponds to the approximate area of one FOV in a 10x microscope objective.

Chip layer alignment: On top of the bottom layer, the lower channel layer (with O-ring) was aligned with the middle layer. Nitrocellulose (NC) (Whatman Protran 0.1) or Polycarbonate (PC) (Sterlitech Polycarbonate [PCTE] Filter Membrane Black 0.1) membranes were cut with 3 mm puncher and inserted on top of the O-ring. The upper channel layer was aligned on top of the middle layer such that the vertical channel aligns precisely over the membrane. A 34 × 24 mm coverslip with 0.15 mm thickness (ThermoFisher) was placed on top of the upper channel layer. All layers, together with the cover slip, were clamped with a milled PMMA frame (CAD drawings available on request) containing an imaging window, fitting 10x and 20x microscope objectives, inserts for tube connections and screw inlets for clamping (Supplementary Figure S1). A summary of different membranes that were tested, and their properties, can be found in Supplementary Table S2. All chip layers can be reused by rinsing in 70% Ethanol and 2x in Milli-Q $H_2O$ and re-assembled with a fresh membrane.

### Generation of circular templates and RCA products

All oligonucleotides used in this study were produced by IDT (Belgium and USA), a list of the oligonucleotide sequences used can be found in Table 1 and Supplementary Table S3. Circular templates were generated by performing a padlock probe ligation reaction templated by a single-stranded DNA (ssDNA) synthetic target (Figure 1 A1.2). A ligation mix, composed of 10 nM PA padlock probe, 30 nM PA synthetic target, T4 ligase reaction buffer (66 mM Tris-HCl (pH 7.5), 10 mM DTT, 10 mM $MgCl_2$, DNA-Gdansk), 0.2 μg/μl BSA, 0.68 mM ATP (DNA-Gdansk) and 1 U T4 ligase (DNA-Gdansk) in 100 μl reaction volume, was incubated at 37°C for 20 min. The reaction was heat inactivated at 65°C for 2 min. Ligated circles were diluted and amplified by a target- primed RCA reaction composed of 100 pM ligated circles (concentration estimated on the initial padlock probe concentration), 0.2 μg/μl BSA, ϕ29 polymerase reaction buffer (33 mM Tris-acetate pH-7.9, 10 mM Mg-acetate, 66 mM K-acetate, 0.1% (v/v), Tween 20, 1 mM DTT, Thermo Scientific), 125 μM dNTPs (DNA Gdansk) and 0.2 U/μl ϕ29 polymerase (Olink, Sweden), which was incubated at 37°C for 60 min and 65°C for 2 min for enzyme heat inactivation.

RCA products were fluorescently labelled by hybridization of short fluorescently tagged complementary detection probe (Figure 1 A1.4). For that purpose, RCA products were first diluted to 10 pM and then 50 μl RCA products were mixed with 50 μl 2x labelling buffer containing 20 mM Tris-HCl (pH 8.0), 20 mM ethylenediaminetetraacetic acid (EDTA), 0.10% Tween-20, 2 M NaCl and 10 nM of fluorescently tagged oligonucleotide generating a final RCA product concentration of 5 pM. The hybridization reaction was incubated for 2 min at 75°C and 10 min at 55°C.

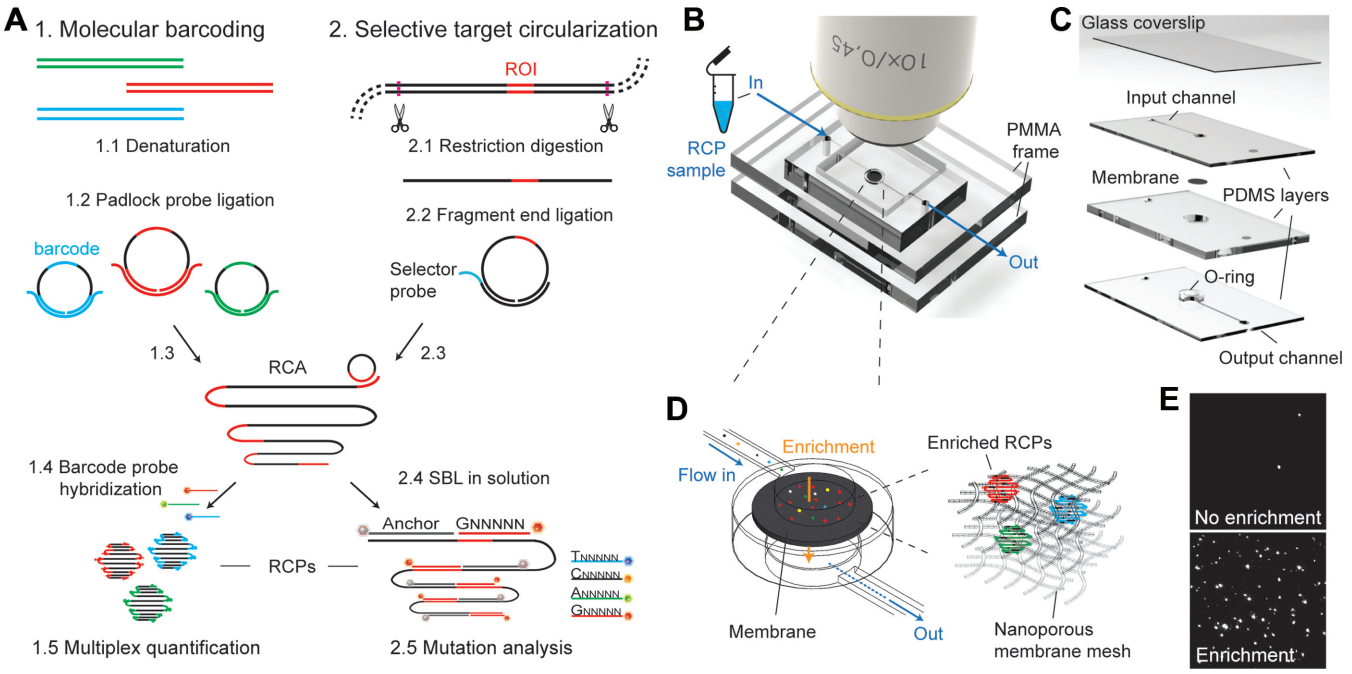


**Figure 1.** Single-molecule analysis through microfluidic enrichment of rolling circle amplification products. (**A**) Sample preparation and target detection by generation of circular templates: (1) Molecular barcoding of DNA through ligation of barcoded target-specific padlock probes, (2) selective circularization of digested genomic DNA fragments through sequence end-complementary selector probes. 1.3 and 2.3.: Circularized molecules are clonally amplified through RCA, generating micron-sized DNA coils that can be fluorescently labelled through (1.4) hybridization of barcode complementary fluorescent probes, or (2.4) base-specific ligation of sequencing by ligation (SBL) interrogation probes in solution. Universal anchor probes with AlexaFluo750 label (illustrated in grey) guides identification of RCPs; SBL interrogation probes carry base-specific fluorescent labels that, after specific ligation to the anchor probe, permit nucleotide identification. (**B**) Assembled RCP enrichment microfluidic chip is placed directly under conventional low magnification fluorescent microscope objectives. (**C**) Exploded view of the multilayer PDMS microfluidic chip outlining microfluidic channels and the embedded membrane (detailed information about the assembly can be found in Supplementary Figure S1). (**D**) Close-up scheme of the interfaced flow cell with embedded membrane that captures RCPs when solutions are flowed through the chip. To the right: Schematic illustration of how RCPs are captured in the nano-porous membrane mesh by a combination of size exclusion and adsorption within the membrane fibres surface. (**E**) Selected FOV regions within images of a solution of RCPs analysed on a microscope slide without enrichment (top) and on a membrane after enrichment (bottom).

### Determination of the dynamic range

In order to measure the detection efficiency of our microfluidic enrichment methodology and compare it to state-of-the-art RCP detection methods, serial RCP dilutions were prepared and quantified through (i) standard microscope slides, (ii) ASMD in flow read-out and (iii) microfluidic enrichment. For that purpose, the final concentration of a prepared RCP solution was determined by standard quantification on microscope slides and subsequent calculation of the detectable RCP concentration (Supplementary Note S1 and Supplementary Table S4). RCPs were prepared at a theoretical concentration of 5 pM (based on the given padlock probe concentration determined by the oligo vendor), as described in the previous method section. The RCP concentration was then quantified in duplicates by applying 10 μl RCP solution onto a positively charged microscope slide (Superfrost plus, VWR) and covering the solution with a 24 × 24 mm cover slip (Menzel, ThermoFisher), spreading out RCPs over the entire area under the cover slip. After 5 min incubation at RT, RCPs were adsorbed to the glass slide and were imaged with a 10x objective (FOV = 1.33 × 1.33 mm). For this, six randomly chosen positions under the coverslip were imaged, quantified and the average number of RCPs/FOV was calculated. The final concentration was estimated taking into account the total number of FOV/coverslip and extrapolated to the total volume (Supplementary Note S1 and Supplementary Table S4).

Seven serial log dilutions were then prepared in 1x labelling buffer (10 mM Tris-HCl pH-8.0, 10 mM EDTA, 0.05% Tween-20, 1 M NaCl). Quantification through amplified single molecule detection in flow was performed using the Aquila 400 instrument (Q-linea, Sweden) (5), where 50 μl RCP dilutions were analysed in duplicates. Images were acquired and automatically analysed by the Aquila 400 custom software. Quantification through microfluidic enrichment was performed by flowing 50 μl RCP dilutions in duplicates through the microfluidic RCP enrichment chip at 50 μl/min with a syringe pump (New Era Pump Systems, Inc.). After enrichment, the membranes were removed from the chip and imaged with a Zeiss Axio Imager Z2 at 10x magnification. All images were analysed with CellProfiler 2.1.2 (Broad Institute) (20) with a pipeline optimized for RCP quantification using adaptive thresholding, robust background method and automatic size of smoothening filter for de-clumping (Pipeline is available on request).

**Table 1.** Representative set of oligonucleotide sequences used in this study. The complete list can be found in Supplementary Table S3

| Oligonucleotide | Sequence (5' to 3' direction with end specific modifications) |
|---|---|
| **PA Synthetic Target** | AGGCCTTTACCCCACCAACTAGCTAATCCGACCTAGGCTCATCTGATAGC GTGAGGTCCGAAGATCCCC**CACTTTCTCCCTCAGGACGTATGCGGTA** |
| **PA Padlock probe** | $PO_4$- **AGGGAGAAAGTG**AGAGTGTATGCAGCTCCTCAGTATAGTCGATAGTCAC GGCTACTTTT**CCGCATACGTCCTG** |
| **Detection probe for PA RCPs** | Cy3-AGTCGATAGTCACGGCTACT |
| ***KRAS* MseI selector** | TTTTTTTTTTTT**AGAACATGTCACACATAAGGTTAAAACAAGATTTACCTC TATTGTTGG**TTTTT |
| ***KRAS* synthetic MseI fragment** | $PO_4$- **TAACCTTATGTGTGACATGTTCT**AATATAGTCACATTTTCATTATTTTTATT ATAAGGCCTGCTGAAAATGACTGAATATAAACTTGTGGTAGTTGGAGCT**G GTGGC**GTAGGCAAGAGTGCCTTGACGATACAGCTAATTCAGAATCATTTT GTGGACGAATATGAT**CCAACAATAGAGGTAAATCTTGTTT** |
| **Anchor Primer for *KRAS* selector RCPs** | AlexaFluor750 - UGUGGUAGUUGGAGCU |

Target complementary regions are highlighted in bold; detection oligonucleotides or anchor primer hybridization sites are marked in green; *KRAS* codons 12 and 13 are marked in bold red and underline base corresponds to the mutated position.

### Co-localization of RCPs

RCPs (1 pM) differentially labelled with FITC and Cy3, were mixed in a ratio of 1:1 and subsequently enriched on a NC membrane in the microfluidic chip. The membrane was removed from the chip and imaged by a Zeiss LSM 710 confocal microscope. Images at different focal depths and co-localization of RCPs were quantified using the same CellProfiler pipeline as described above, but adding the RelateObjects analysis module to calculate the distance and co-localization between identified objects in different confocal images. Moreover, five image sets with simulated random distribution of RCPs were generated by exporting image data with ImageJ to a .txt file, randomly re-distributing RCP positions assuming an object size of 1–4 pixels$^2$. Finally, the generated randomized data sets were imported into ImageJ and exported as TIFF images that were analysed with the same CellProfiler pipeline for co-localization, as described above.

For membrane penetration depth analysis of RCPs and Cy3 labelled T1 MyOne beads (Dynal Thermo Fisher), confocal images were exported and analysed separately by a customized MATLAB script with intensity threshold 20 and size filtering 2–20 for RCPs, and 40 and 4–40, for fluorescent beads, respectively.

### Identification of pathogens by barcoded padlock-probe ligation

Padlock probes were designed to detect species-specific DNA sequences from three bacterial pathogens: *Escherichia coli*, *Staphylococcus aureus* and *Pseudomonas aeruginosa*, and 2 antibiotic resistance markers: OXA-48 and *mecA*, for carbapanem and methicillin resistance, respectively (Supplementary Table S3, Supplementary Table S5). Each padlock probe contained a unique molecular barcode that allowed barcode-specific fluorescent labelling of RCPs (Figure 1A, Supplementary Table S3). Bacterial genomic DNA was obtained by extraction from cultured strains by the guanidium thiocyanate method (21). To determine the sensitivity and the dynamic range of the padlock probe-RCA assay in solution, a log dilution series in Milli-Q $H_2O$ from 100 to 0.1 pg/μl of *S. aureus* genomic DNA was prepared. Ten microlitres of each dilution was denatured and fragmented during 5 min at 95°C and put on ice immediately. Padlock probe ligation was done by adding 100 pM *S. aureus* padlock probe in 1x Ampligase buffer (20 mM Tris-HCl (pH 8.3), 25 mM KCl, 10 mM $MgCl_2$, 0.5 mM NAD and 0.01% Triton® X-100, Epicenter) and 0.25 U/μl Ampligase (Epicenter) in a final volume of 20 μl. Ligation was performed at 55°C for 40 min. The obtained circles were directly subjected to target-primed RCA without prior purification. For that purpose, 20 μl RCA mix was directly added to the 20 μl circles. RCA was performed with the same conditions as described above, but with an amplification time of 120 min. RCP labelling was performed under the same conditions as described above, using the barcode specific detection oligonucleotides (Supplementary Table S3) at a final concentration of 10 nM each in a final volume of 60 μl.

For the multiplexed detection of different pathogens and corresponding antibiotic resistance markers, samples with different compositions were prepared diluting bacterial ge-

nomic DNA to ∼1 ng (Supplementary Table S5). The samples were subjected to the assay using a cocktail of all padlock probes during ligation at 100 pM each. To validate the specificity of the multiplexed assay in the presence of background DNA, a mix with bacterial genomic DNA of closely related pathogens, *Staphylococcus haemolyticus, Staphylococcus epidermidis, Pseudomonas putida and Pseudomonas oleovarans* at ∼10 ng each, and human genomic DNA (∼125 ng) was prepared. One nanogram bacterial genomic DNA of the species targeted by the padlock probe panel, were added to the background DNA mix and the prepared samples were subjected to the assay described above.

All resulting RCP solutions were flowed and enriched through the microfluidic chip in a NC membrane using the conditions described in the determination of the dynamic range. Image acquisition and analysis were performed as described in previous sections.

### Selector probe assay and single-base sequencing by ligation in solution

For the quantification of mutations through microfluidic enrichment, we implemented a selector probe-based approach, as outlined in Figure 1A2. Selector probes are described in detail elsewhere (22,23). In brief, we designed *Mse*I *KRAS* gene fragment specific selector probes that selectively template the circularization of 192 base long *Mse*I DNA fragments of the *KRAS* gene that are obtained after enzymatic digestion of genomic DNA with *Mse*I restriction endonuclease. For that purpose, the *KRAS Mse*I selector probes contain a 50 base long sequence that is complementary to the last 25 bases on both, the 5′ and the 3′ end of the *Mse*I *KRAS* DNA fragment (Table 1, Supplementary Table S3). Synthetic *Mse*I *KRAS* DNA fragments were circularized by ligation upon hybridization of the fragment ends on the *KRAS Mse*I selector probes (Figure 1A2), in a ligation mix composed of Ampligase reaction buffer (20 mM Tris-HCl (pH 8.3), 25 mM KCl, 10 mM $MgCl_2$, 0.5 mM NAD and 0.01% Triton® X-100, Epicenter), 0.25 U/μl Ampligase (Epicenter) in a final volume of 20 μl ligation, incubated at 55°C for 30 min. For the analysis of samples with low ratios of mutant DNA fragments amongst a majority of wild-type DNA sequences, short *KRAS* fragments with wild type and codon 12 point mutation sequences were mixed in increasing ratios (1:1, 1:10, 1:100 and 1:1000) and ligated on the short fragment selector probe (Supplementary Table S3). The circles were diluted to 10 pM and then amplified through RCA, primed by the 3′ end of the selector probe using the same RCA conditions as described above.

Generated RCPs were then subjected to a single base sequencing by ligation (SBL) reaction directly in solution (Figure 1A2.4) (24,25), interrogating the first nucleotide of codon 12 in the KRAS gene. First, 30 μl RCPs were labelled with a *KRAS* sequence specific anchor primer (Alexa750 labelled) by addition of 10 μl 2x phi29 buffer with 5 nM anchor primer final concentration and incubation at 75°C for 2 min and 55°C for 10 min. Anchor primer stained RCPs were then mixed with 10 μl SBL reaction mix containing 0.2 μg/μl BSA, 0.25 mM ATP and 50 nM SBL interrogation probes (see Supplementary Table S3), and 100 mU/μl final concentration T4 Ligase (DNA Gdansk). The mix was incubated at RT for 60 min and followed by incubation at 65°C for 1 min to inactivate the enzyme. The in solution sequenced RCPs were enriched on PC membranes with the microfluidic enrichment method, imaged and analysed with a custom-made CellProfiler and MATLAB-based sequencing analysis pipeline that was described previously (26).

## RESULTS

### Single-molecule counting scheme

We base our approach on targeted sample preparation schemes that allow converting single NA molecules into circular amplification substrates with high target specificity and multiplexing capability, combined with RCA directly in solution. DNA targets are either: (i) barcoded through specific ligation of barcoded padlock probes (4,27), or (ii) selectively circularized through target specific selector probes (22) (Figure 1A). Circularized DNA molecules are then clonally amplified through RCA, generating micron-sized DNA amplicons that maintain the single molecule integrity in solution due to intermolecular repulsion (28). RCPs can be labelled with a range of colorimetric, magnetic or fluorescent labels. Yet, the highest level of multiplexing capability and cost-effectiveness is achieved by hybridization of barcode complementary fluorescently tagged oligonucleotide probes (Figure 1A1.4). Here, we also subject RCPs to a single base SBL reaction directly in solution that enables simple targeted single nucleotide variation (SNV) analysis (Figure 1A2.4).

For enrichment, we designed a multilayer PDMS microfluidic device with an embedded nano-porous membrane (Figure 1B–D, Supplementary Figure S1). RCP solutions are flowed through the chip with simple fluidic control. While passing through the membrane, RCPs are captured, most likely through a combination of size exclusion and adsorption on the surface of the membrane mesh, favoured by the high affinity of the NC surface to large ssDNA molecules (29,30) (Figure 1D). As a result, RCPs are enriched into a reduced analysis area that corresponds to one FOV of a 10x magnification objective of a standard fluorescent microscope (Figure 1B–D). RCP enrichment significantly increases the detector occupancy compared to standard microscope slide read-out (no enrichment, Figure 1E), and state-of-the-art RCP quantification methods (Supplementary Figure S2).

### Microfluidic RCP enrichment enables high sensitivity digital read-out

To determine the quantitative dynamic range of our microfluidic RCP enrichment method, we prepared a 6 log-dilution series ranging from $1.9 \times 10^{-13}$ M to $1.1 \times 10^{-19}$ M RCPs (measured and estimated by quantification on microscope slides as described in Supplementary Note S1 and Supplementary Table S4). We then analysed 50 μl of each dilution using our microfluidic RCP enrichment method (Figure 2A and B), and compared the performance to conventional microscope slide read-out (no enrichment, Figure 2A and C), and ASMD RCP quantification (Figure 2D). Performances are compared in detail in Supplementary Figure S3. Using our microfluidic enrichment method,

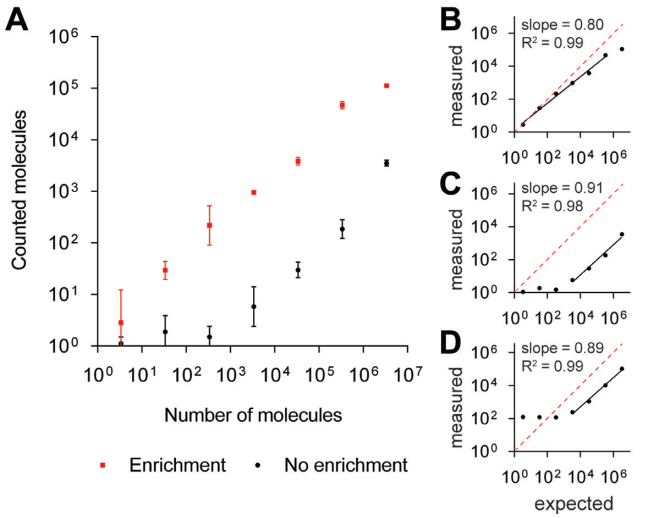


**Figure 2.** Single-molecule counting performance. (**A**) Quantification range of microfluidic RCA products (RCP) enrichment (red) compared to no enrichment (black). The counted number of RCP molecules on Y axis is plotted against the expected number of RCP molecules on the X axis, estimated as described in Supplementary Note S1. Error bars ±1 st. dev. of the mean, n = 2. (**B**–**D**) Measured RCP counts are plotted against the expected RCP counts in a log-dilution series using (B) enrichment, (C) no enrichment and (**D**) state-of-the-art RCP quantification in flow (Aquila 400, Q-linea). Black solid lines indicate linear fit to the linear response data points. Slopes and $R^2$ values of linear fits are plotted in the figures. Red dashed lines indicate the maximum dose response.

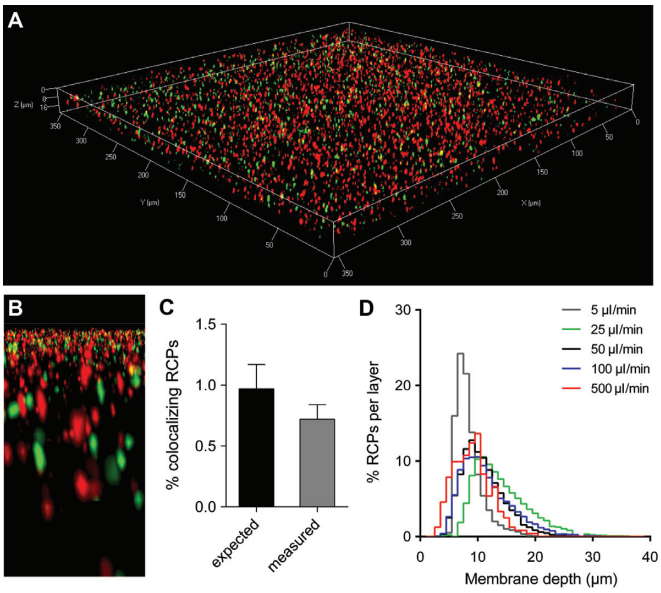


**Figure 3.** Enriched RCPs at high concentration can be resolved via confocal microscopy. (**A**) 3D rendered confocal Z stack of 1 pM RCPs labelled with either Cy3 or FITC, and enriched on a NC membrane. (**B**) A detailed 3D rendered region inside the membrane with Cy3 and FITC labelled RCPs. (**C**) Co-localization measurement of enriched RCPs and expected numbers of co-localization by chance. Artificial images with objects with random distributions and the same number, size and intensity of the measured RCPs were generated and co-localization were measured with the same parameters (Error bars ±1 st. dev. of the mean, n = 5 for random images, n = 3 for measured RCP images). (**D**) Distribution of RCP localization inside the membrane as a function of different flow rates used during enrichment.

we observed a high RCP capture efficiency, with corresponding detection efficiencies of up to 82% of the expected molecule counts (Figure 2A and B, Supplementary Note S1 and Supplementary Table S4). We measured the limit-of-detection at 1.2 aM RCP concentration and obtained a dynamic quantification range over 5 orders of magnitude up to 190 fM (Figure 2A and B and Supplementary Table S4).

The sensitivity of our microfluidic enrichment analysis method is substantially higher than the previously reported RCA detection methods (Supplementary Table S1). The overall performance of our RCA-based single-molecule counting scheme compares well with commercially available digital single-molecule analysis systems (Table 2), however, it is significantly simpler, more cost-effective and can be performed with standard laboratory equipment.

We observed a decreasing dose response at elevated concentrations (slope = 0.8, Figure 2B). We investigated whether this is caused by optical resolution limitations, or by RCP aggregation induced by the enrichment (Figure 3). We observed that RCPs can penetrate into the membrane and be immobilized to a depth of ∼30 μm (Figure 3A, B and D), while rigid particles do not penetrate the membrane to the same extent (Supplementary Figure S4A). This can probably be attributed to the flexibility of coiled ssDNA. The membrane penetration depth is mostly unaffected by flow speed (Figure 3D), whereas at high concentrations, RCPs tend to penetrate deeper into the membrane (Supplementary Figure S4B). Confocal microscopy of membranes enriched with a high concentration of two different RCP populations labelled with either Cy3 or FITC fluorescent labels (Figure 3A and B), revealed only 0.72% (±0.12) co-localized objects, which is below the expected number of co-localizing RCPs assuming a random spatial distribution (Figure 3C). This is in line with previous reports demonstrating RCP repulsion in homogeneous solution (28,31), and demonstrates that at high concentration, microfluidic enrichment does not lead to RCP aggregation, but to dense RCP alignment in 3D. To improve the dose response at low magnification, thinner membranes, such as track etched PC, can be used to align RCPs in 2D (slope 0.98, Supplementary Figure S3 and Supplementary Note S2).

## Detection of bacterial pathogens and drug resistance markers

In order to demonstrate the analytical utility of RCP enrichment for detecting NA targets, we employed the detection system in combination with a multiplex padlock probe assay to detect DNA from bacterial pathogens. In a simple 4-step sample preparation procedure, extracted bacterial DNA was first heat denatured, padlock probes ligated, amplified by RCA and labelled by hybridizing fluorescently tagged detection probes complementary to the species-specific barcode sequences in the RCPs, as outlined in Figure 1A1–1.4. The sequential addition of reagents during the assay steps increases the sample volume and dilutes the initial target concentration, and hence, requires enrichment to achieve sensitive detection. In order to determine the dynamic range of RCP enrichment under these assay conditions, log dilutions of extracted bacterial genomic

**Table 2.** Comparison of digital NA quantification methods

| | Dynamic range | Sensitivity (concentration) | Multiplexing capability | Cost/ Required instrumentation |
|---|---|---|---|---|
| RCP enrichment | 5 logs | 1.2 aM | 5-plex* | Low/standard fluorescent microscope |
| Digital PCR (BioRAD) | 5 logs | 1.6 aM (37,38) | 2-plex | High/three instruments for droplet generation, PCR and droplet read-out |
| Nanostring | 6 logs | 100 aM (6) | 800-plex | High/two instruments for sample preparation and digital analyzer |
| NGS | 4-6 logs depending on library prep. and seq depth | ∼0.5–30% molecule detection efficiency depending on library prep. and seq depth (9,39,40) | Not limited | High/diverse sample prep. equipment, complex library prep. schemes and expensive NGS reagents and instrument |

*Multiplexing capacity can be increased by using sequential hybridization or NGS schemes (25,26).

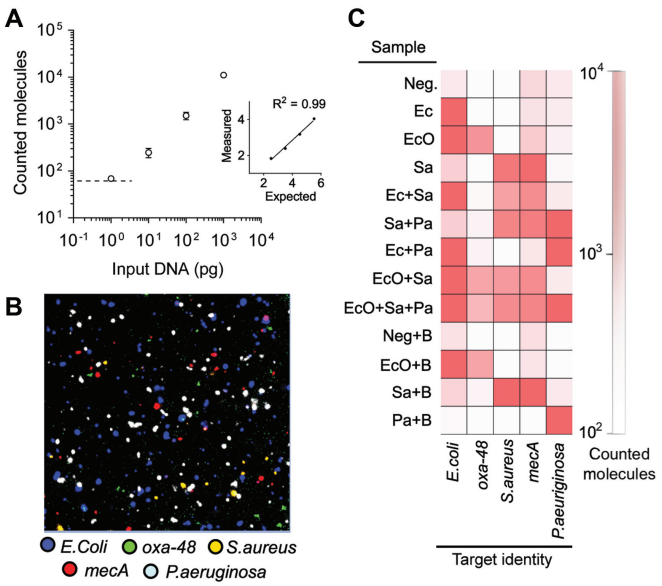


**Figure 4.** Multiplex quantification of pathogenic bacterial DNA and associated antibiotic resistance markers. (**A**) Dilutions of *S. aureus* genomic DNA were subjected to padlock probe ligation, RCA, specific RCP labelling and microfluidic RCP enrichment analysis (Error bars ±1 st. dev. of the mean, n = 2). Dashed line illustrates the limit of detection at 61 RCPs (calculated as negative control + 3 st. dev. from the mean). Inset graph shows linear fit of log expected versus log measured molecule count ($R^2$ = 0.99). (**B**) Representative region of an image after enrichment of processed sample mix containing *E. coli*/oxa-48 (EcO), *S. aureus*/*mecA* (Sa) and *P. aeruginosa* (Pa). Fluorescent colour code representing the different padlock probe DNA targets is depicted under the image. (**C**) Multiplex pathogen and antibiotic marker detection. RCP counts per sample and padlock probe DNA targets are illustrated as a heat map. Samples with 'B' correspond to mixes with added background DNA. For raw RCP counts and additional negative controls see Supplementary Table S6.

DNA from a cultured strain of *S. aureus* were prepared, subjected to the assay and analysed by our microfluidic enrichment method (Figure 4A). As little as 1 pg genomic DNA (∼300 copies) was detected, without the need for any pre- or additional amplification steps.

The detection sensitivity of this assay format is currently limited by the number of fluorescent objects detected in the negative control (40 ± 7). However, unlike the dynamic range determination with pre-labelled diluted RCPs (Figure 2), the labelling step in this assay format comprises a higher concentration of fluorescent detection probes that pass through the membrane and may contribute to increased background signals. In ligase- and RCA negative control experiments, similar signal counts were obtained, as in the fluorescent labelling mix itself, suggesting that the background signals mostly arise from fluorescent detection probe aggregates in the labelling mix (Supplementary Table S6).

Next, we set up a multiplex assay that targets three different pathogens and two corresponding antibiotic resistance markers including common etiological agents of hospital-acquired infections (32). Padlock probes were designed with specific molecular barcode sequences, enabling simultaneous identification of species and antibiotic resistance markers using five different fluorescent barcode detection probes (Figures 1A and 4B). We then analysed samples containing different pathogenic genomic DNAs (Figure 4C, Supplementary Table S6). All pathogens and respective resistance marker genes were accurately identified (Figure 4C, Supplementary Table S6). To prove the robustness of the assay in complex samples, we analysed the pathogenic genomic DNA in samples with a high background of human genomic DNA and bacterial genomic DNA of closely related bacteria. We detected all targeted pathogens with the same specificity as when using a pure bacterial DNA sample, and observed no signal increase in negative controls (Figure 4C, last 4 rows), underlining the specificity of the assay in complex samples.

## Oncogene rare mutation analysis

We further demonstrate the versatility of our digital NA analysis method by quantifying a mutation in the oncogene *KRAS*. We designed a *KRAS* specific selector probe assay to specifically circularize and amplify *KRAS* DNA fragments by RCA, as outlined in Figure 1A2. To interrogate SNVs within the individual KRAS-RCPs, we developed and optimized a single base SBL reaction for KRAS-RCPs in solution (Figure 5A, Supplementary Table S7). When using ASMD RCP analysis (Supplementary Figure S5A–B), and when using quantification on microscope slides, the read-out of in-solution SBL on RCPs was impeded by low signal-to-noise (SNR) ratios, since excess of fluorescent

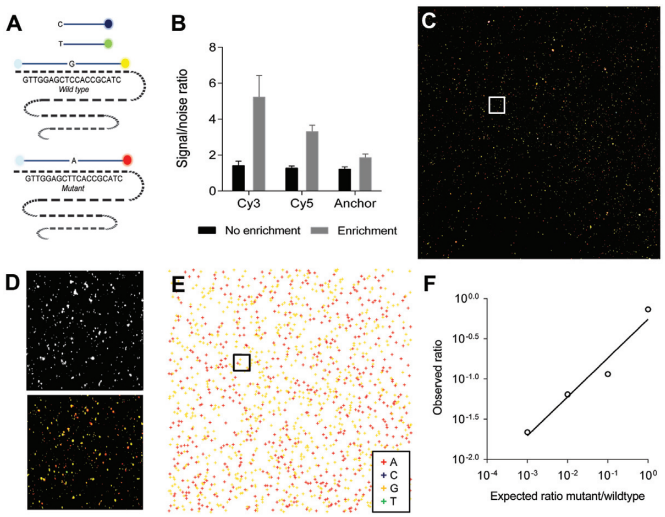


**Figure 5.** Microfluidic enrichment analysis purifies RCPs interrogated by in solution SBL and enables accurate single nucloetide variation (SNV) counting. (**A**) *KRAS* oncogene codon 12 wild type and mutant synthetic DNA fragments were selectively circularized through selector probes, amplified through RCA and SNVs are interrogated by in solution single base SBL. (**B**) Improvement of SNR ratio after purification through RCP enrichment on PC membranes (Error bars ±1 st. dev. of the mean, n = 10 for RCPs and background pixels. (**C**) Enriched RCPs of equimolar mixtures (1:1) of wild type (Cy3 label) and mutant (Cy5 label) DNA fragments. (**D**) Subset of image in C showing fluorescent anchor primer (Alexa750) in white (top) and combined image of the four fluorescent channels (bottom) representing the interrogated base-specific staining for base A (Cy5), C (Texas Red), G (Cy3) and T (Alexa488). (**E**) SNV analysis of individual RCPs through in-house developed image processing script with base calling algorithm is plotted, with KRAS mutant RCPs as red objects and KRAS wild-type RCPs as yellow objects. (**F**) RCPs from KRAS wild type and mutant fragments were mixed in different ratios: 1:1, 10:1, 100:1, 1000:1, enriched and imaged on PC membranes. Expected ratio of SNVs for different ratios of mutant/wild-type mixes is plotted versus the measured ratio.

SBL probes were not removed (Figure 5B). Similarly, upon enrichment on NC membranes, fluorescent SBL probes accumulated in the membrane and decreased the SNR ratio (Supplementary Figure S5C). To overcome this limitation, we utilized un-charged PC membranes for enrichment of SBL-interrogated RCPs, through which excess SBL probes were removed, significantly increasing the SNR ratio (Figure 5B). A detailed performance characterization of RCP enrichment on PC membranes can be found in Supplementary Note S2 and Supplementary Figures S6 and S7.

Synthetic DNA fragments with KRAS wild-type sequence and *KRAS* fragments with a codon 12 point mutation were mixed in different ratios (1:1, 1:10, 1:100 and 1:1000) and subjected to the selector probe-RCA assay. Enrichment analysis of SBL-interrogated RCPs on PC membranes allowed for accurate SNV discrimination (Figure 5C–E). Rare mutant fragments mixed in wild-type fragments in ratios down to 1:1000 were successfully detected (Figure 5F), suggesting the feasibility of our digital NA analysis method for rare mutation analysis.

## DISCUSSION

We have developed a fundamentally novel digital analysis strategy that allows single molecule counting with a conventional low magnification fluorescence microscope. Single molecule analyses has gained in popularity as they provide higher quantitative precision and sensitivity than bulk analogue measurements. Moreover, analysing molecules at an individual level enables discrimination of rare molecule aberrations, such as SNVs, that would not be detectable in bulk measurements. While virtually every laboratory is equipped with PCR thermocyclers and gel electrophoresis devices for read-out, the broad implementation of digital assays is limited by the high cost associated with new instrumentation that has to be acquired to perform digital analysis (10). In contrast, our digital analysis method can be performed with standard laboratory equipment. RCP enrichment is achieved through a simple three-layer PDMS microfluidic chip with a vertically embedded membrane (Figure 1B–D, Supplementary Figure S1). We want to highlight that the simplicity of the microfluidic chip design does not require any clean room facilities for manufacturing or accurate flow control instruments for fluidic handling. The flow speed during enrichment has no substantial effects on the efficiency (Figure 3D and Supplementary Figure S7), suggesting that even manual pipetting may be sufficient. Therefore, our method enables performing digital NA analysis in any laboratory equipped with a conventional fluorescent microscope. Despite its simplicity and cost-effectiveness, the performance of our digital analysis method compares well with commercially available solutions (Table 2).

RCA has since long been demonstrated as a suitable single molecule detection technique that can be used to amplify thousands of circular templates in multiplex, without need for compartmentalization (33). RCA is also used to clonally amplify whole genome library preparations and generate billions of NGS substrates in a single reaction tube (25). In combination with padlock and selector probes, RCA has been used for the precise quantification of copy number variations, gene expression and detection of a wide range of pathogenic microorganisms (5,13,16,34). We believe that the reason for the limited use of RCA for NA quantification has mainly been due to the lack of a simple and efficient read-out. State-of-the art RCP quantification methods are strongly limited by the occupancy of RCPs on the sensor area per time unit (Supplementary Figure S2) resulting in low detection efficiencies, and consequently, in detection limits in the femto-molar range (Supplementary Table S1 and Supplementary Figure S3) (5,28,31). Here, we have substantially increased the number of RCPs on the sensor area by enriching RCPs into a single FOV of a 10x magnification objective of a conventional fluorescent microscope (Figure 1E and Supplementary Figure S2). RCP enrichment increases the occupancy on the detector by ∼50 fold, which in turn increases the RCP detection efficiency up to 82% and consequently increases the sensitivity to the attomolar range (Figure 2, Supplementary Figure S3). As the main mechanism of RCP capture in NC membranes relies on a combination of size exclusion and adsorption, we cannot exclude the possibility that smaller RCPs may leak through the 100 nm pore sized mesh of the membrane. However,

these RCPs would not be detectable in the filtrate, because RCPs of such small size consist of only few copies of the barcode sequence and, hence, only carry few fluorescent labels. It is important to note that we have taken this into consideration when calculating the efficiency of RCP enrichment. The number of detectable RCPs, carrying sufficient numbers of fluorophores to be detected, was determined with the same imaging settings as in the membrane enrichment experiments (Supplementary Note S1).

To our knowledge, this is the highest RCP sensitivity reported so far (for a detailed comparison to other reported digital RCP quantification methods, see Supplementary Table S1). The high sensitivity of our enrichment method enables specific and sensitive molecular identification, and quantification of pathogens together with antibiotic resistance markers in a very simple assay configuration. Accurate multiplex detection was achieved in a total assay time, from purified DNA to result, of 3.5 h (Figure 1A1, Figure 4). Similarly, an onogene mutation was detected in low frequency using in solution SBL on RCPs and subsequent enrichment analysis (Figure 1A2, Figure 5), with a performance comparable to other digital quantification techniques (10).

Interestingly, we found that our RCP enrichment method has the capacity to immobilize RCPs in membranes at a density higher than by random distribution (Figure 3). The observed, lower than expected, dose response (slope 0.8) and saturation at $\sim 10^5$ RCPs/FOV occurs due to the limitation in optical resolution of low magnification standard fluorescent microscopy (Figure 2A). Confocal imaging with higher magnification facilitates resolving RCPs at even higher density (Figure 3A–C), and could potentially extend the dynamic range even further. Drmanac *et al*. developed a high density DNA nanoball sequencing array that aligns RCPs, generated in solution on an ordered array, significantly increasing the RCP density compared to that of random alignment on a flat surface, and hence increasing sequencing throughput (25). Densely packing RCPs through microfluidic enrichment on membranes may be a promising alternative for generating even denser sequencing arrays in 3D. Our microfluidic chip could thus be used as a flow cell, in which enriched RCPs, spatially immobilized in a high-density 3D array, are interrogated by NGS chemistries.

We achieved better sensitivity when detecting diluted preformed RCPs (Figure 2), compared to genomic DNA dilutions subjected to the multiplex assay (Figure 4). The decreased assay sensitivity is due to inefficiencies during sample preparation, probe ligation and RCP formation, which we estimated has an efficiency of ∼22% (Supplementary Note S1). Moreover, a measurable level of background is caused by fluorophore and detection probe aggregates (Supplementary Table S6). To further increase the sensitivity, the sample preparation efficiency can be increased by improving target fragmentation and template-directed ligation efficiencies. Elimination of fluorophore aggregates through pre-filtration and/or ultra-sonication may help to decrease the background signal and, hence, lower the limit of detection. Additionally, the simple chip design may allow parallelization of multiple enrichment channels and the analysis of multiple samples simultaneously in conventional microscope slide or even 96-well plate formats. Upgrading the chip architecture may improve the image acquisition on-chip, which will allow using sequential hybridization and NGS chemistries, opening up for highly multiplexed and targeted NA sequencing analysis.

Altogether, microfluidic RCP enrichment provides a versatile platform for NA digital quantification analysis, allowing wider implementation of digital assays in any laboratory. In combination with miniaturized sample preparation devices (35,36), and due to its simplicity, it has the potential to be integrated into micro total analysis systems for a wide range of applications in research and diagnostics.

## SUPPLEMENTARY DATA

Supplementary Data are available at NAR Online.

## ACKNOWLEDGEMENT

The authors thank Dr Pieter Moons from University of Antwerp for providing extracted genomic DNAs from bacterial strains used in this study. The authors would also like to thank Dr Narayanan Srinivasan for comments on the manuscript.

## FUNDING

European Commission's Seventh Framework Programme [FP7/2007-2013 under BIOMAX project 264737]; Innovative Medicine Initiative [RAPP-ID grant agreement, no. 115153]; The Ecole Polytechnique Fédérale de Lausanne and the EU Ideas program [ERC-2012-AdG-320404 to M.C. and M.G.]; Swedish Foundation for Strategic Research (SSF) [Flu-ID project No. SBE13-0125]; The Swedish Research Council (VR); Formas Strong Research Environment [Biobridges, project no. 221-2011-1692]; Innovative Medicines Initiative 2 joint Undertaking [115843 to EbolaMoDRAD project] supported by the European Union's Horizon 2020 research and innovation programme and EFPIA. Funding for open access charge: Swedish Foundation for Strategic Research (SSF) grant [Flu-ID project No. SBE13-0125]; The Swedish Research Council (VR); Formas Strong Research Environment [Biobridges, project no. 221-2011-1692]; Innovative Medicines Initiative 2 joint Undertaking [115843 to EbolaMoDRAD project].
*Conflict of interest statement.* None declared.

## REFERENCES

1. Sykes,P.J., Neoh,S.H., Brisco,M.J., Hughes,E., Condon,J. and Morley,A.A. (1992) Quantitation of targets for PCR by use of limiting dilution. *Biotechniques*, **13**, 444–449.
2. Vogelstein,B. and Kinzler,K.W. (1999) Digital PCR. *Proc. Natl. Acad. Sci. U.S.A.*, **96**, 9236–9241.
3. Lizardi,P.M., Huang,X., Zhu,Z., Bray-Ward,P., Thomas,D.C. and Ward,D.C. (1998) Mutation detection and single-molecule counting using isothermal rolling-circle amplification. *Nat. Genet.*, **19**, 225–232.
4. Banér,J., Nilsson,M., Mendel-Hartvig,M. and Landegren,U. (1998) Signal amplification of padlock probes by rolling circle replication. *Nucleic Acids Res.*, **26**, 5073–5078.
5. Jarvius,J., Melin,J., Göransson,J., Stenberg,J., Fredriksson,S., Gonzalez-Rey,C., Bertilsson,S. and Nilsson,M. (2006) Digital quantification using amplified single-molecule detection. *Nat. Methods*, **3**, 725–727.

6. Geiss,G.K., Bumgarner,R.E., Birditt,B., Dahl,T., Dowidar,N., Dunaway,D.L., Fell,H.P., Ferree,S., George,R.D., Grogan,T. *et al.* (2008) Direct multiplexed measurement of gene expression with color-coded probe pairs. *Nat. Biotechnol.*, **26**, 317–325.
7. Mitra,R.D. and Church,G.M. (1999) In situ localized amplification and contact replication of many individual DNA molecules. *Nucleic Acids Res.*, **27**, e34.
8. Xu,L., Brito,I.L., Alm,E.J. and Blainey,P.C. (2016) Virtual microfluidics for digital quantification and single-cell sequencing. *Nat. Methods*, **13**, 759–762.
9. Kivioja,T., Vaharautio,A., Karlsson,K., Bonke,M., Enge,M., Linnarsson,S. and Taipale,J. (2012) Counting absolute numbers of molecules using unique molecular identifiers. *Nat. Methods*, **9**, 72–74.
10. Huggett,J.F., Cowen,S. and Foy,C.A. (2015) Considerations for digital PCR as an accurate molecular diagnostic tool. *Clin. Chem.*, **61**, 79–88.
11. Zhong,Q., Bhattacharya,S., Kotsopoulos,S., Olson,J., Taly,V., Griffiths,A.D., Link,D.R. and Larson,J.W. (2011) Multiplex digital PCR: breaking the one target per color barrier of quantitative PCR. *Lab Chip*, **11**, 2167–2174.
12. Fire,A. and Xu,S.Q. (1995) Rolling replication of short DNA circles. *Proc. Natl. Acad. Sci. U.S.A.*, **92**, 4641–4645.
13. Göransson,J., Wählby,C., Isaksson,M., Howell,W.M., Jarvius,J. and Nilsson,M. (2009) A single molecule array for digital targeted molecular analyses. *Nucleic Acids Res.*, **37**, e7.
14. Sato,K., Tachihara,A., Renberg,B., Mawatari,K., Sato,K., Tanaka,Y., Jarvius,J., Nilsson,M. and Kitamori,T. (2010) Microbead-based rolling circle amplification in a microchip for sensitive DNA detection. *Lab Chip*, **10**, 1262–1266.
15. Kühnemund,M. and Nilsson,M. (2014) Digital quantification of rolling circle amplified single DNA molecules in a resistive pulse sensing nanopore. *Biosens. Bioelectron.*, **67**, 1–7.
16. Göransson,J., Ke,R., Nong,R.Y., Howell,W.M., Karman,A., Grawé,J., Stenberg,J., Granberg,M., Elgh,M., Herthnek,D. *et al.* (2012) Rapid identification of bio-molecules applied for detection of biosecurity agents using rolling circle amplification. *PLoS One*, **7**, e31068.
17. Tanaka,Y., Xi,H., Sato,K., Mawatari,K., Renberg,B., Nilsson,M. and Kitamori,T. (2011) Single-molecule DNA patterning and detection by padlock probing and rolling circle amplification in microchannels for analysis of small sample volumes. *Anal. Chem.*, **83**, 3352–3357.
18. Dahl,F., Banér,J., Gullberg,M., Mendel-Hartvig,M., Landegren,U. and Nilsson,M. (2004) Circle-to-circle amplification for precise and sensitive DNA analysis. *Proc. Natl. Acad. Sci. U.S.A.*, **101**, 4548–4553.
19. Shrirao,A.B., Hussain,A., Cho,C.H. and Perez-Castillejos,R. (2012) Adhesive-tape soft lithography for patterning mammalian cells: application to wound-healing assays. *Biotechniques*, **53**, 315–318.
20. Kamentsky,L., Jones,T.R., Fraser,A., Bray,M.-A., Logan,D.J., Madden,K.L., Ljosa,V., Rueden,C., Eliceiri,K.W. and Carpenter,A.E. (2011) Improved structure, function and compatibility for CellProfiler: modular high-throughput image analysis software. *Bioinformatics*, **27**, 1179–1180.
21. Pitcher,D.G., Saunders,N.A. and Owen,R.J. (1989) Rapid extraction of bacterial genomic DNA with guanidium thiocyanate. *Lett. Appl. Microbiol.*, **8**, 151–156.
22. Dahl,F., Gullberg,M., Stenberg,J., Landegren,U. and Nilsson,M. (2005) Multiplex amplification enabled by selective circularization of large sets of genomic DNA fragments. *Nucleic Acids Res.*, **33**, e71.
23. Dahl,F., Stenberg,J., Fredriksson,S., Welch,K., Zhang,M., Nilsson,M., Bicknell,D., Bodmer,W.F., Davis,R.W. and Ji,H. (2007) Multigene amplification and massively parallel sequencing for cancer mutation discovery. *Proc. Natl. Acad. Sci. U.S.A.*, **104**, 9387–9392.
24. Shendure,J. (2005) Accurate multiplex polony sequencing of an evolved bacterial genome. *Science*, **309**, 1728–1732.
25. Drmanac,R., Sparks,A.B., Callow,M.J., Halpern,A.L., Burns,N.L., Kermani,B.G., Carnevali,P., Nazarenko,I., Nilsen,G.B., Yeung,G. *et al.* (2010) Human genome sequencing using unchained base reads on self-assembling DNA nanoarrays. *Science*, **327**, 78–81.
26. Ke,R., Mignardi,M., Pacureanu,A., Svedlund,J., Botling,J., Wählby,C. and Nilsson,M. (2013) In situ sequencing for RNA analysis in preserved tissue and cells. *Nat. Methods*, **10**, 857–860.
27. Nilsson,M., Malmgren,H., Samiotaki,M., Kwiatkowski,M., Chowdhary,B.P. and Landegren,U. (1994) Padlock probes: circularizing oligonucleotides for localized DNA detection. *Science*, **265**, 2085–2088.
28. Blab,G.A., Schmidt,T. and Nilsson,M. (2004) Homogeneous detection of single rolling circle replication products. *Anal. Chem.*, **76**, 495–498.
29. Van Oss,C.J., Good,R.J. and Chaudhury,M.K. (1987) Mechanism of DNA (southern) and protein (western) blotting on cellulose nitrate and other membranes. *J. Chromatogr. A*, **391**, 53–65.
30. Gillespie,D. (1968) [148]The formation and detection of DNA-RNA hybrids. *Methods Enzymol.*, **12**, 641–668.
31. Melin,J., Jarvius,J., Göransson,J. and Nilsson,M. (2007) Homogeneous amplified single-molecule detection: Characterization of key parameters. *Anal. Biochem.*, **368**, 230–238.
32. Tong,S.Y.C., Davis,J.S., Eichenberger,E., Holland,T.L. and Fowler,V.G. (2015) Staphylococcus aureus infections: epidemiology, pathophysiology, clinical manifestations, and management. *Clin. Microbiol. Rev.*, **28**, 603–661.
33. Hardenbol,P., Banér,J., Jain,M., Nilsson,M., Namsaraev,E.A., Karlin-Neumann,G.A., Fakhrai-Rad,H., Ronaghi,M., Willis,T.D., Landegren,U. *et al.* (2003) Multiplexed genotyping with sequence-tagged molecular inversion probes. *Nat. Biotechnol.*, **21**, 673–678.
34. Mezger,A., Gullberg,E., Göransson,J., Zorzet,A., Herthnek,D., Tano,E., Nilsson,M. and Andersson,D.I. (2015) A general method for rapid determination of antibiotic susceptibility and species in bacterial infections. *J. Clin. Microbiol.*, **53**, 425–432.
35. Cui,F., Rhee,M., Singh,A. and Tripathi,A. (2015) Microfluidic sample preparation for medical diagnostics. *Annu. Rev. Biomed. Eng.*, **17**, 267–286.
36. Gan,W., Zhuang,B., Zhang,P., Han,J., Li,C. and Liu,P. (2014) A filter paper-based microdevice for low-cost, rapid, and automated DNA extraction and amplification from diverse sample types. *Lab Chip*, **14**, 18–21.
37. Hindson,C.M., Chevillet,J.R., Briggs,H.A., Gallichotte,E.N., Ruf,I.K., Hindson,B.J., Vessella,R.L. and Tewari,M. (2013) Absolute quantification by droplet digital PCR versus analog real-time PCR. *Nat. Methods*, **10**, 1003–1005.
38. Pinheiro,L.B., Coleman,V.A., Hindson,C.M., Herrmann,J., Hindson,B.J., Bhat,S. and Emslie,K.R. (2012) Evaluation of a droplet digital polymerase chain reaction format for DNA copy number quantification. *Anal. Chem.*, **84**, 1003–1011.
39. Casbon,J.A., Osborne,R.J., Brenner,S. and Lichtenstein,C.P. (2011) A method for counting PCR template molecules with application to next-generation sequencing. *Nucleic Acids Res.*, **39**, e81.
40. Fu,G.K., Xu,W., Wilhelmy,J., Mindrinos,M.N., Davis,R.W., Xiao,W. and Fodor,S.P.A. (2014) Molecular indexing enables quantitative targeted RNA sequencing and reveals poor efficiencies in standard library preparations. *Proc. Natl. Acad. Sci. U.S.A.*, **111**, 1891–1896.